6. Forces on Objects Immersed in a Fluid Flow

The force acting on an object immersed in a fluid flow is comprised of the force due to pressure variations over the surface and the force due to viscous shear stresses.

If we know the pressure (p) and shear stress (τ) distribution over the object, then:

$$\mathbf{F}_P = \int_A -p\hat{\mathbf{n}}dA$$

$$F_{S,i} = \int_A \tau_{ji} n_i dA$$

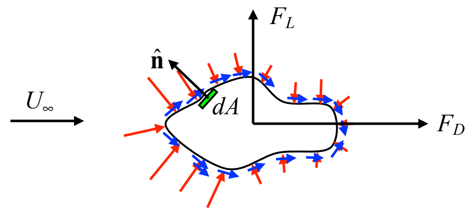

where $\mathbf{F}_P$ is the force due to the pressure component, $\mathbf{F}_S$ is the force due to the shear stress component, and A is the surface area of the object.

The component of the force acting in the direction parallel to the incoming flow is known as the drag force, F_D, and the component perpendicular to the incoming flow is known as the lift force, F_L.

Notes:

1. The pressure force component of the drag is known as form drag while the shear stress drag component is known as the skin friction drag.

2. A streamlined body is one in which the (skin friction drag) >> (form drag).

A bluff body is one in which the (form drag) >> (skin friction drag).

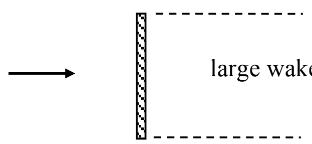

3. The lift and drag are often expressed in dimensionless form as a lift and drag coefficient, C_D and C_L:

$$C_L = \frac{F_L}{\frac{1}{2}\rho U_\infty^2 A} \qquad C_D = \frac{F_D}{\frac{1}{2}\rho U_\infty^2 A}$$

where A is usually the frontal projected area (area seen from the front) for a bluff body or the planform area (the area seen from above) for a streamlined body.

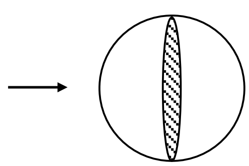

bluff body
(use the frontal projected area)

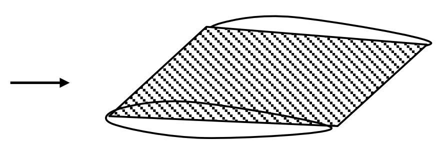

streamlined body
(use the planform area)

Flow Around a Cylinder (or Sphere) As a Function of Reynolds Number

Note: $\text{Re} = \dfrac{VD}{\nu}$

Re << 1
(creeping or Stoke's flow)

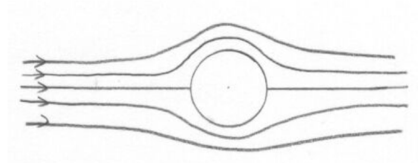

5 < Re < 50
(fixed eddies)

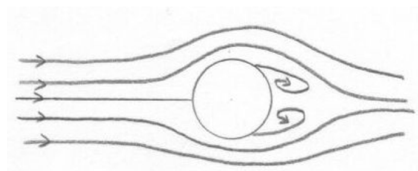

60 < Re < 5000
(Karman Vortex Street,
periodic shedding of vortices)

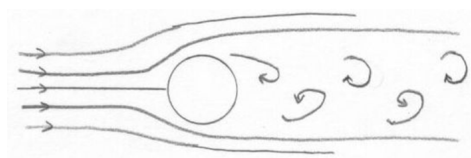

5000 < Re < 200,000

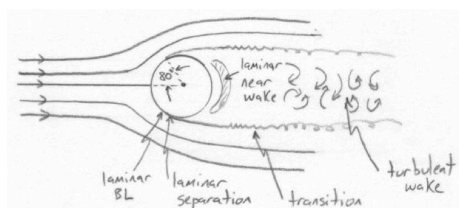

Re ≈ 200,000
(drag crisis)

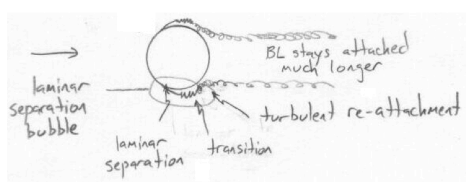

Re > 200,000

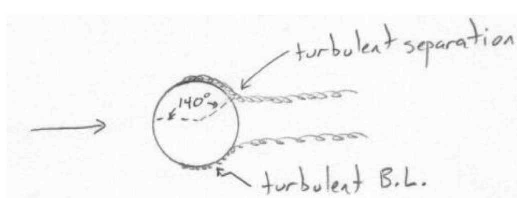

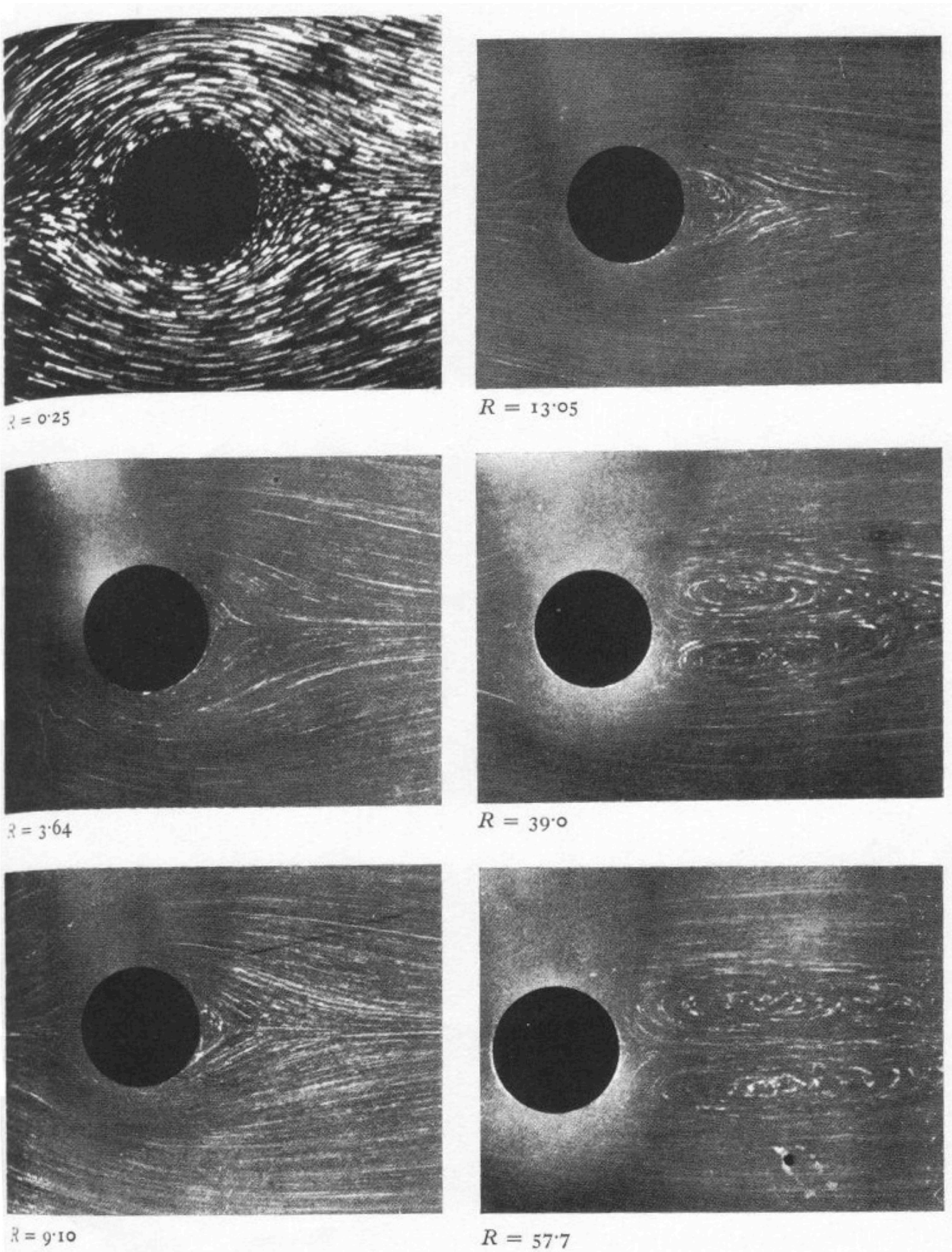

Figure 4.12.1. Streamlines of steady flow (from left to right) past a circular cylinder of radius a; $R = 2aU/\nu$. The photograph at $R = 0{\cdot}25$ (from Prandtl and Tietjens 1934) shows the movement of solid particles at a free surface, and all the others (from Taneda 1956*a*) show particles illuminated over an interior plane normal to the cylinder axis.

(From Batchelor, G.K., *An Introduction to Fluid Dynamics*, Cambridge University Press.)

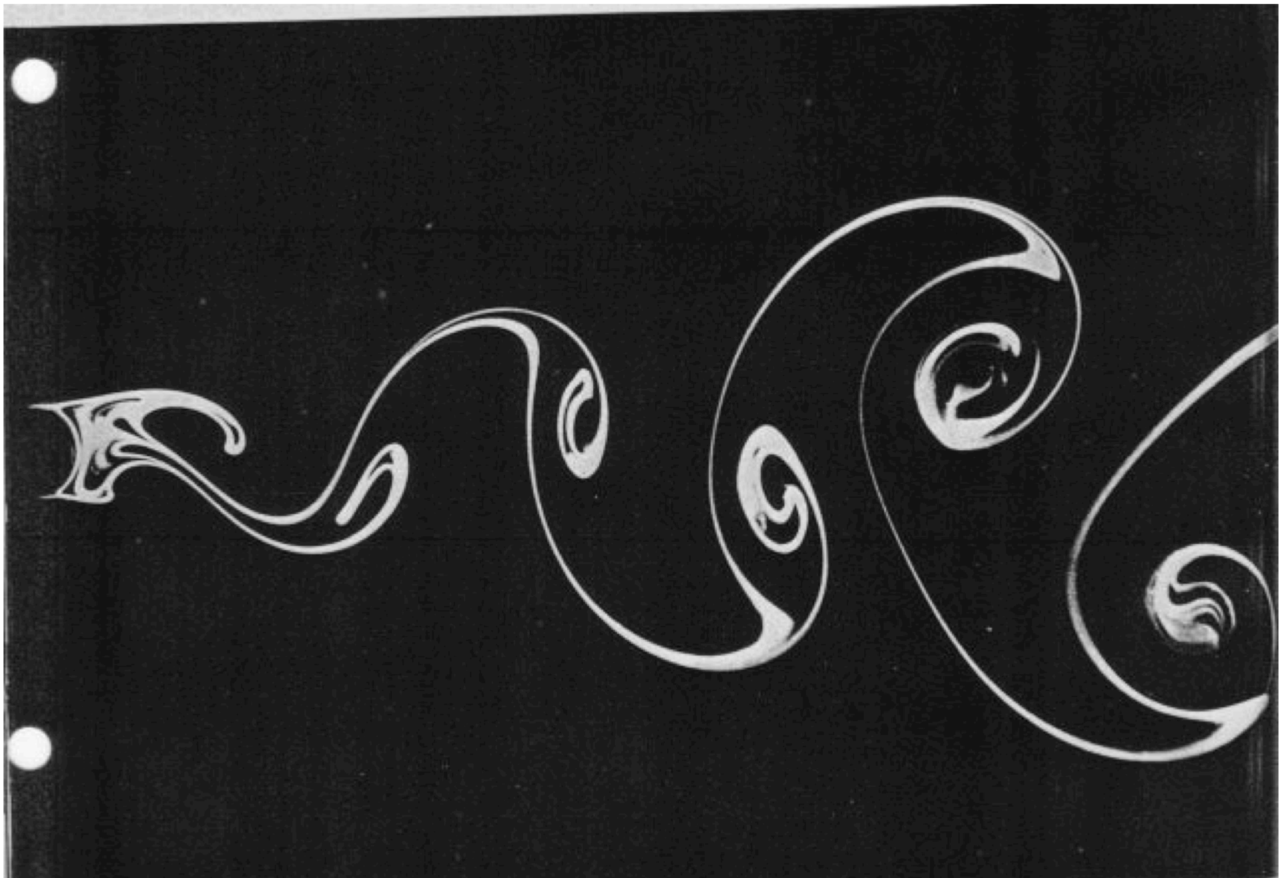

94. Kármán vortex street behind a circular cylinder at $R=140$. Water is flowing at 1.4 cm/s past a cylinder of diameter 1 cm. Integrated streaklines are shown by electrolytic precipitation of a white colloidal smoke, illuminated by a sheet of light. The vortex sheet is seen to grow in width downstream for some diameters. *Photograph by Sadatoshi Taneda*

95. Kármán vortex street behind a circular cylinder at $R=200$. This photograph, made using a different fluid (and in another country) happens to have been timed so as to resemble remarkably the flow pattern in the upper picture. A thin sheet of tobacco smoke is introduced upstream in a low-turbulence wind tunnel. *Photograph by Gary Koopmann*

(From Van Dyke, M., *An Album of Fluid Motion*, Parabolic Press.)

96. **Kármán vortex street behind a circular cylinder at $R=105$.** The initially spreading wake shown opposite develops into the two parallel rows of staggered vortices that von Kármán's inviscid theory shows to be stable when the ratio of width to streamwise spacing is 0.28. Streaklines are shown by electrolytic precipitation in water. *Photograph by Sadatoshi Taneda*

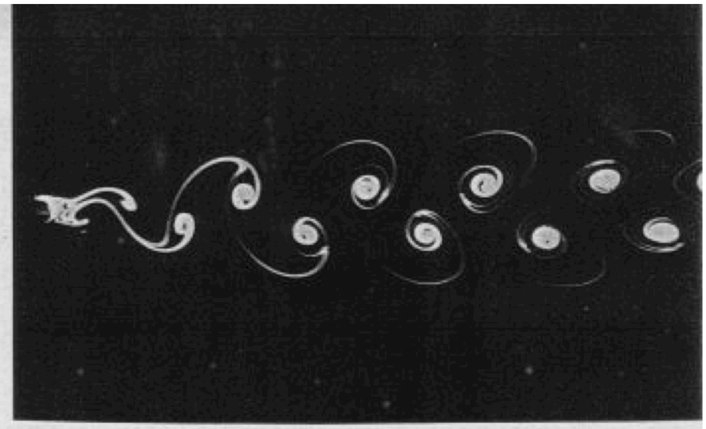

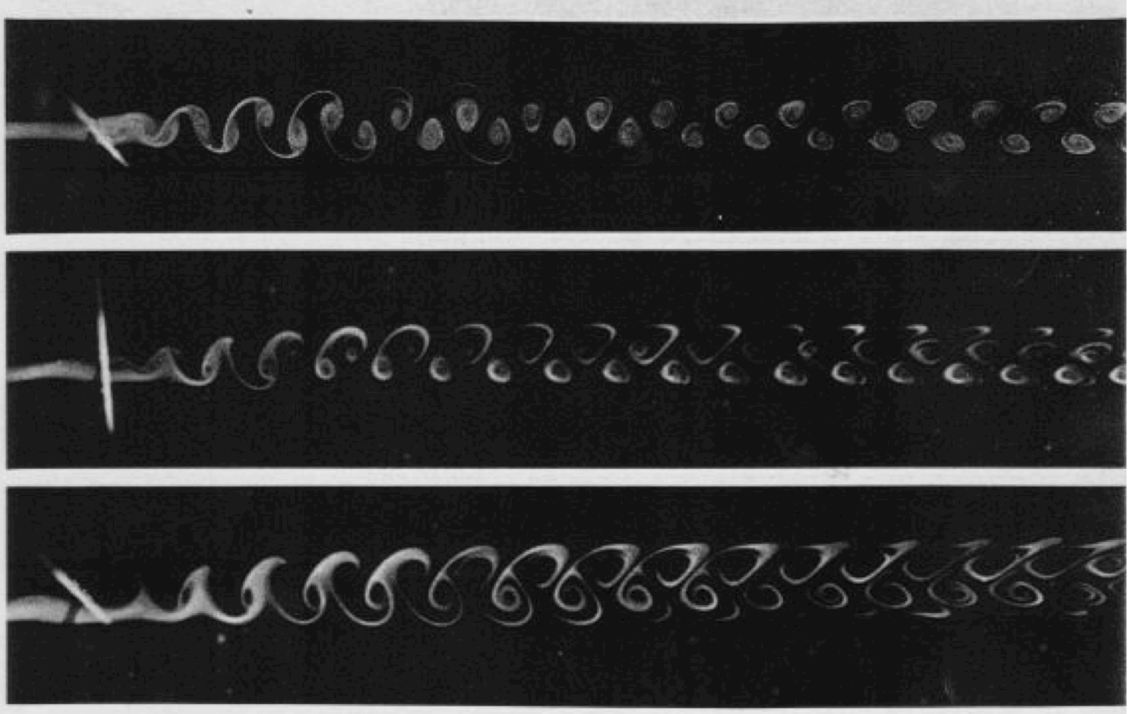

97. **Smoke at various levels in a vortex street.** A smoke filament in air shows, at a Reynolds number of 100, both shear layers (top photographs), only one shear layer (middle), and the irrotational flow below the wake (bottom). *Zdravkovich 1969*

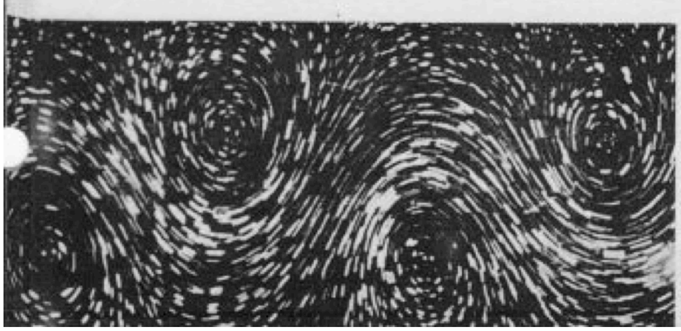

98. **Kármán vortices in absolute motion.** Here the camera moves with the vortices rather than the cylinder. The streamline pattern closely resembles the inviscid one calculated by von Kármán. The flow is visualized by particles floating on water. *Photograph by R. Wille, from Werlé 1973. Reproduced, with permission, from the* Annual Review of Fluid Mechanics, *Volume 5, © 1973 by Annual Reviews Inc.*

57

(From Van Dyke, M., *An Album of Fluid Motion*, Parabolic Press.)

Notes:

1. The periodic shedding of vortices off the object results in periodic forces exerted on the object in the cross-stream direction. The Tacoma Narrows bridge disaster (figure shown below) occurred because a structural natural frequency of the bridge matched the frequency of the shedding vortices.

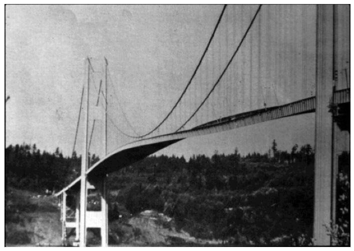

The Tacoma Narrows bridge collapsed in 1940.

2. Experimental measurements have shown that the dimensionless frequency of the shedding vortices, *f*, expressed as a Strouhal number, i.e., St = *fD*/*V*, remains relatively constant at 0.2 for $100 < Re_D < 1*10^6$.

St = *fV*/*D*

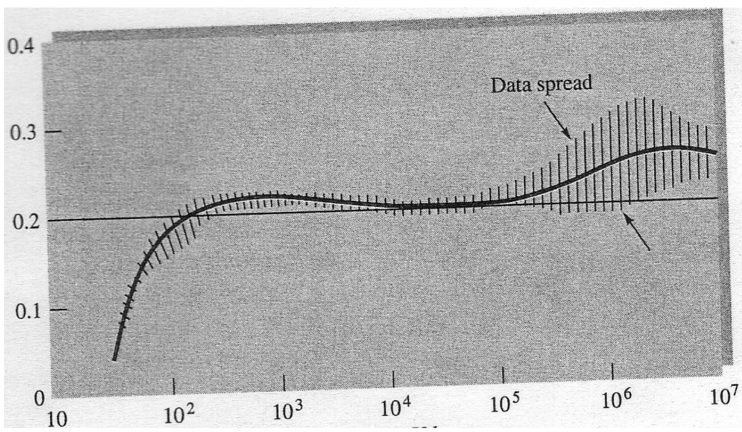

Re = *VD*/ν

(Figure from White, F.M., *Fluid Mechanics*, McGraw-Hill.)

The fact that the Strouhal number is insensitive to the Reynolds number over a wide range of Reynolds numbers has been used to design a flow velocity meter known as the vortex flow meter (shown below).

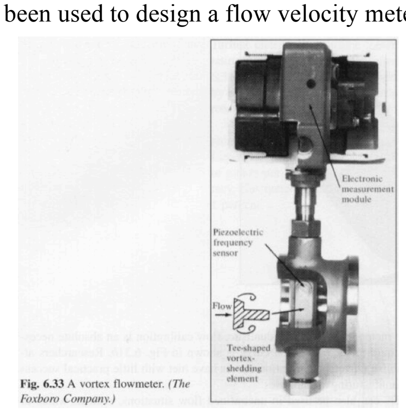

Fig. 6.33 A vortex flowmeter. *(The Foxboro Company.)*

By measuring the frequency of the forces acting on the obstruction (of known size) and knowing that the Strouhal number is approximately equal to 0.2, the flow velocity can be estimated.

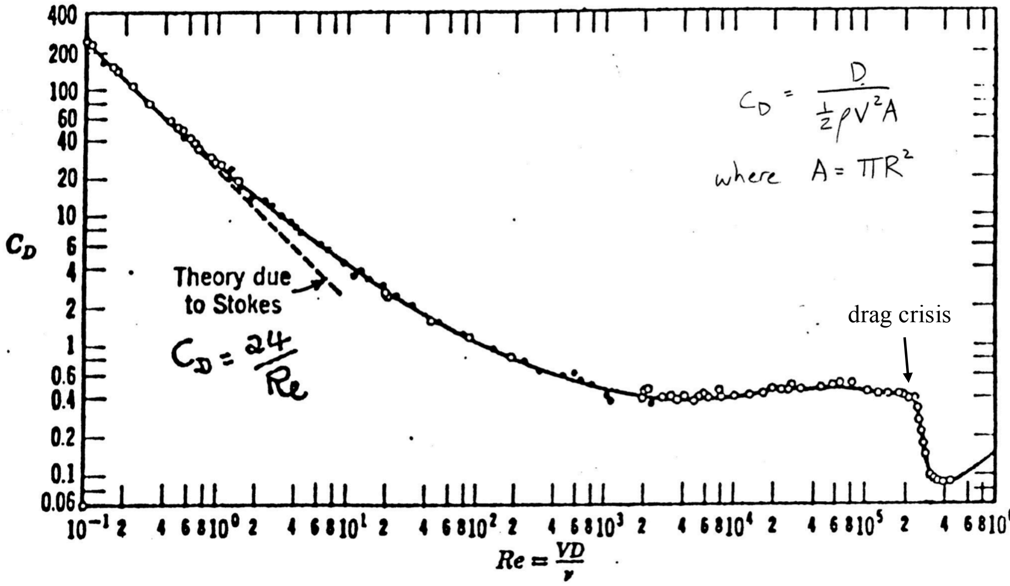

Fig. 8.32 Drag coefficient of a sphere as a function of Reynolds number (Ref. 13).

Commonly used curve fits to the curve shown above are:

$Re_D < 1$:	C_D	=	$24/Re_D$ (Stokes' drag law)
$Re_D < 5$:	C_D	=	$24/Re_D\,(1+3/16Re_D)$ (Oseen's approximation)
$0 \le Re_D \le 2*10^5$:	C_D	=	$24/Re_D + 6/(1+Re_D^{0.5}) + 0.4$
$Re_D < 2*10^5$:	C_D	=	0.44 (Newton's Law)

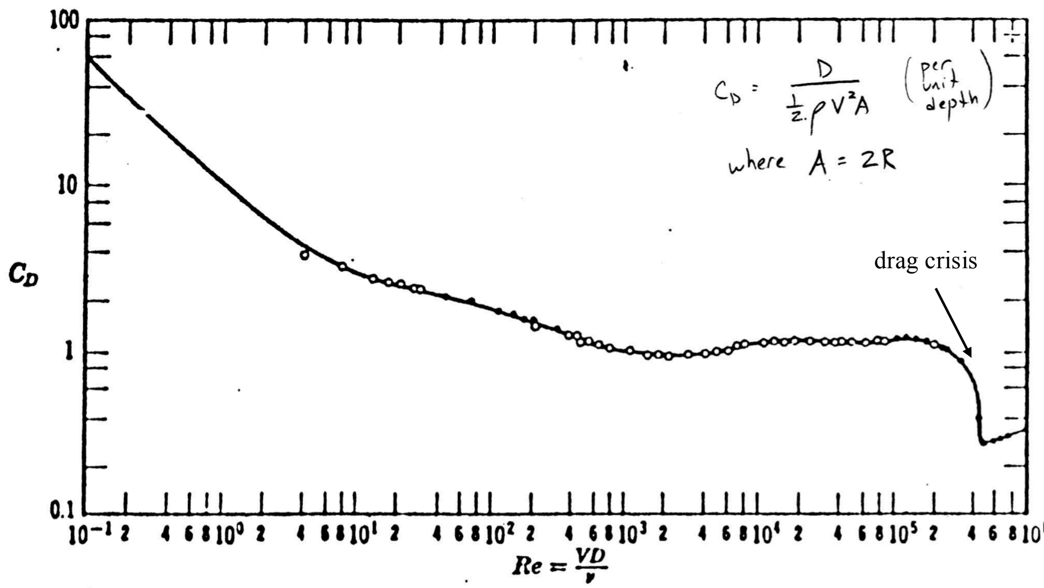

Fig. 8.34 Drag coefficient for circular cylinders as a function of Reynolds number (Ref. 13).

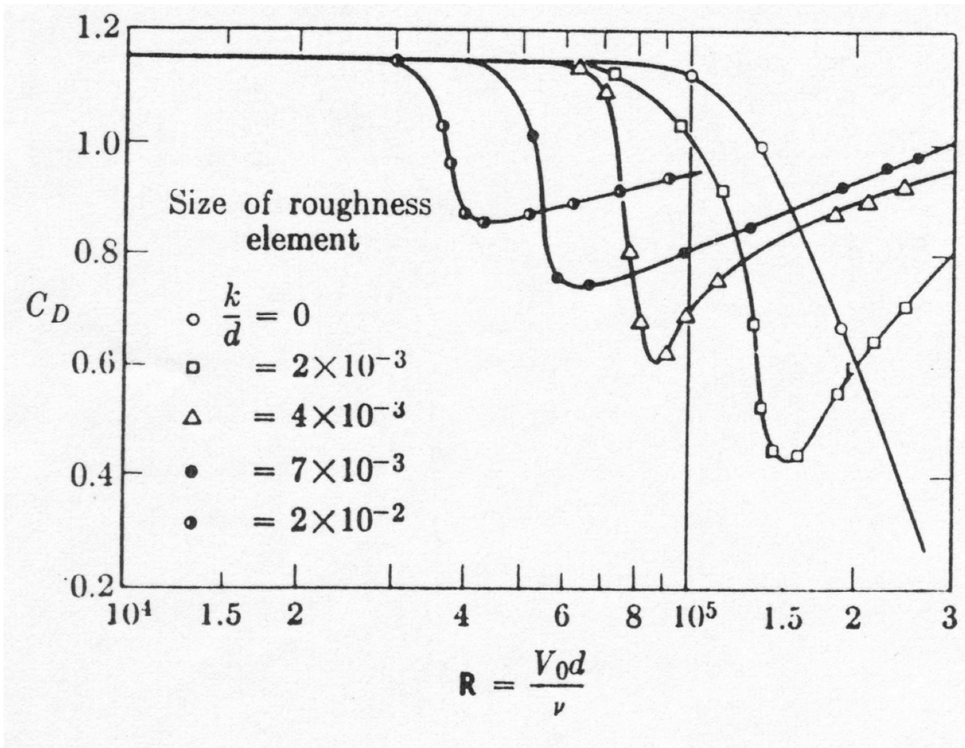

FIG. 15–9. Drag on circular cylinders of varying roughness [10].

From the data we observe that increasing the roughness of the surface causes the drag crisis to occur at a smaller Reynolds number.

Note:

The Reynolds number for a 95 mph baseball and a 170 mph golf ball are approximately 206,000 and 213,000, respectively. Hence, both are near the drag crisis!

The following is from White, F.M, *Fluid Mechanics*, 3rd ed, McGraw-Hill.

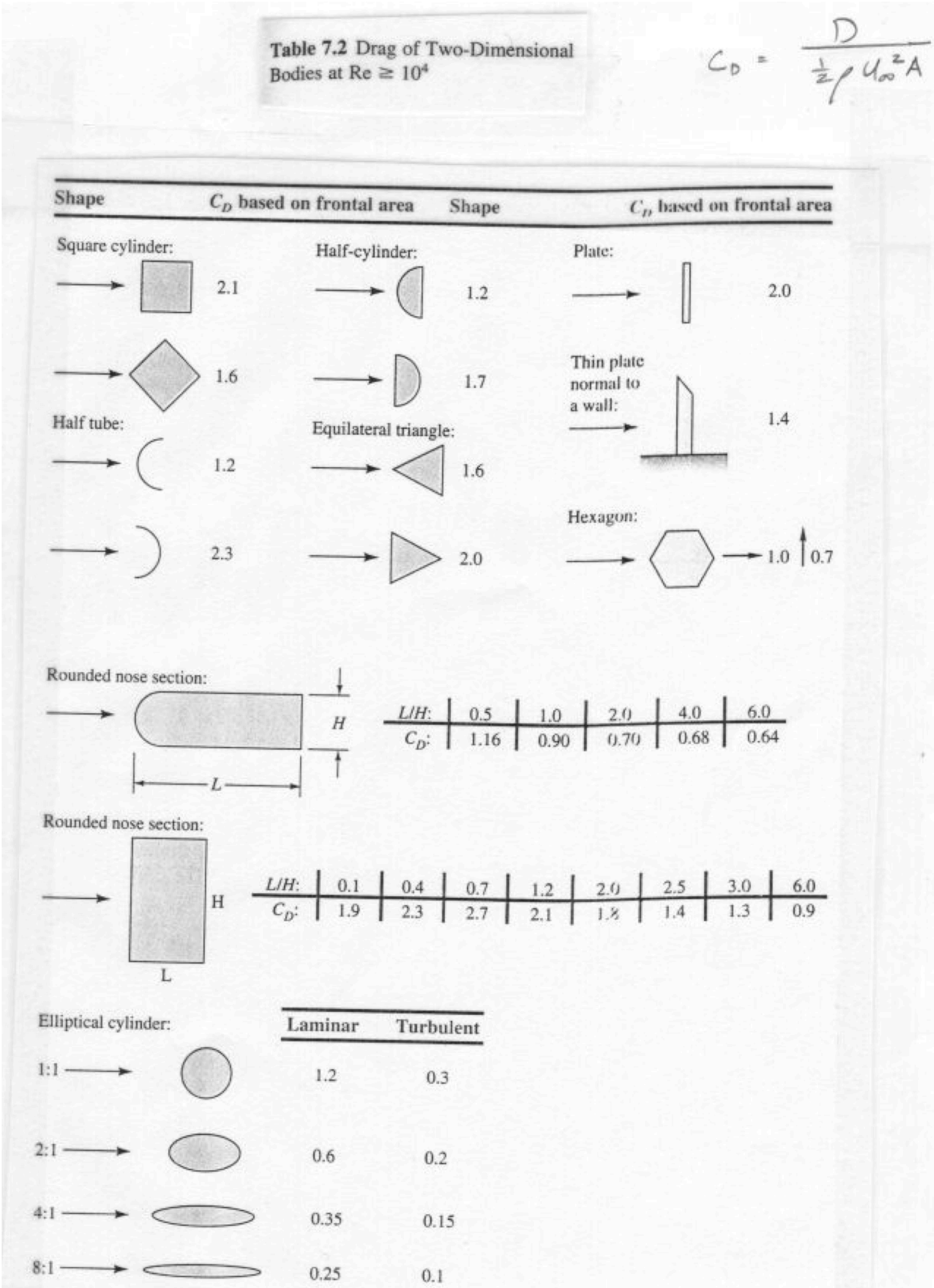

Table 7.2 Drag of Two-Dimensional Bodies at Re ≥ 10^4

$$C_D = \frac{D}{\frac{1}{2}\rho U_\infty^2 A}$$

Shape	C_D based on frontal area	Shape	C_D based on frontal area	Shape	C_D based on frontal area
Square cylinder: (flat face to flow)	2.1	Half-cylinder: (flat face downstream)	1.2	Plate:	2.0
Square cylinder: (corner to flow)	1.6	Half-cylinder: (flat face upstream)	1.7	Thin plate normal to a wall:	1.4
Half tube: (convex side to flow)	1.2	Equilateral triangle: (point to flow)	1.6	Hexagon: (flow →)	1.0
Half tube: (concave side to flow)	2.3	Equilateral triangle: (flat face to flow)	2.0	Hexagon: (flow ↑)	0.7

Rounded nose section: (L, H)

L/H:	0.5	1.0	2.0	4.0	6.0
C_D:	1.16	0.90	0.70	0.68	0.64

Rounded nose section: (L, H)

L/H:	0.1	0.4	0.7	1.2	2.0	2.5	3.0	6.0
C_D:	1.9	2.3	2.7	2.1	1.8	1.4	1.3	0.9

Elliptical cylinder:

	Laminar	Turbulent
1:1	1.2	0.3
2:1	0.6	0.2
4:1	0.35	0.15
8:1	0.25	0.1

The following is from White, F.M, *Fluid Mechanics*, 3rd ed, McGraw-Hill.

Table 7.3 Drag of Three-Dimensional Bodies at Re ≥ 10^4

Body	C_D based on frontal area
Cube: (face to flow)	1.07
Cube: (edge to flow)	0.81
Cup: (concave back)	1.4
Cup: (concave front)	0.4
Disk:	1.17
Parachute (Low porosity):	1.2

Body	C_D based on frontal area							
Cone:	θ:	10°	20°	30°	40°	60°	75°	90°
	C_D:	0.30	0.40	0.55	0.65	0.80	1.05	1.15

Body	C_D based on frontal area								
Short cylinder, laminar flow:	L/D:	1	2	3	5	10	20	40	∞
	C_D:	0.64	0.68	0.72	0.74	0.82	0.91	0.98	1.20

Body	C_D based on frontal area						
Porous parabolic dish [23]:	Porosity:	0	0.1	0.2	0.3	0.4	0.5
	← C_D:	1.42	1.33	1.20	1.05	0.95	0.82
	→ C_D:	0.95	0.92	0.90	0.86	0.83	0.80

Body	C_D based on frontal area
Average person:	→ $C_DA \approx 9\ \text{ft}^2$ ↑ $C_DA \approx 1.2\ \text{ft}^2$

Body	C_D based on frontal area				
Pine and spruce trees [24]:	U, m/s:	10	20	30	40
	C_D:	1.2 ± 0.2	1.0 ± 0.2	0.7 ± 0.2	0.5 ± 0.2

Body	Ratio	C_D based on frontal area
Rectangular plate:	b/h 1	1.18
	5	1.2
	10	1.3
	20	1.5
	∞	2.0

Body	Ratio	C_D based on frontal area
Flat-faced cylinder:	L/d 0.5	1.15
	1	0.90
	2	0.85
	4	0.87
	8	0.99

Body	Ratio	Laminar	Turbulent
Ellipsoid:	L/d 0.75	0.5	0.2
	1	0.47	0.2
	2	0.27	0.13
	4	0.25	0.1
	8	0.2	0.08